ISBN: 978-3-95450-132-8 doi:10.18429/JACoW-IPAC2014-THPME128

FAST BEAM DIAGNOSTICS FOR THIRD-GENERATION SYNCHROTRONS BY MEANS OF NOVEL DIAMOND-BASED PHOTON BPMS

M. Antonelli, G. Cautero, I. Cudin, D. M. Eichert, D. Giuressi, W. H. Jark, E. Karantzoulis, S. Lizzit, R. H. Menk, Elettra – Sincrotrone Trieste S.C.p.A., Trieste, Italy
A. De Sio, E. Pace, Università degli Studi di Firenze, Firenze, Italy
M. Di Fraia, Università degli Studi di Trieste, Trieste, Italy

Abstract

In the past years electron beam stability has been intensively addressed in new-generation Synchrotron Radiation (SR) sources. Many SR machines have been equipped with a Fast Orbit Feedback (FOFB) based on electron Beam-Position Monitors (eBPMs). Also photon Beam-Position Monitors (pBPMs) are a useful tool for keeping the electron beam under control by simultaneously monitoring position and intensity of the delivered radiation; the machine control system can take advantage of this information in order to improve the electron beam stability.

At Elettra, a diagnostic beamline, which utilizes a couple of single-crystal CVD diamond detectors as fast pBPMs, has been built and inserted into a bending-magnet front end. Preliminary tests carried out during normal machine operations show that this system allows monitoring the beam position with sub-micrometric precision at the demanding readout rates required by the FOFB. Therefore, this diagnostic line represents a demonstrator for future implementation of pBPMs at several bending-magnet front ends of Elettra.

INTRODUCTION

Electron-beam monitoring and stabilization are amongst the primary concerns in modern Synchrotron Radiation (SR) facilities. In particular, the high-brightness beamlines using undulator radiation are the most sensitive to electron-beam oscillations occurring in 3rd-generation light sources [1]. Therefore, such machines are equipped with specific control systems, like the Fast Orbit FeedBack (FOFB), based on the measurements of the electron Beam-Position Monitors (eBPMs) implemented along their storage rings [2].

Notwithstanding such stabilization measures, the resulting photon beam can exhibit residual fluctuations in terms of both position and intensity owing to a number of instability sources. These phenomena can be detected by utilizing photon Beam Position Monitors (pBPMs), which allow estimating simultaneously the intensity and the position of the emitted beam passing through. Fast pBPMs inserted in beamlines are well-suited for either *a posteriori* data calibration or real-time adjustment in beamline experiments [3]. Nevertheless, the information provided by such detectors is useful for the electron-beam diagnostics and it can be integrated into the FOFB [4]. In particular, if pBPMs are installed upstream from the beamline optics, their measurements are directly related to the status of the electron beam as they are not affected by any instability imputable to optical elements (such as mirrors, monochromators, etc.).

Amongst the available technologies for the production of fast and semitransparent *in situ* pBPMs, diamond grown by Chemical Vapour Deposition (CVD) is one of the most suitable materials thanks to its outstanding physical properties. Because of its high bond energy it can withstand the high dose rates occurring in 3rd- and 4th-generation SR sources and its low atomic number makes it semitransparent to X-rays. Besides, due to its high energy gap, intrinsic diamond is an insulator with low thermal noise at room temperature, while its high electron and hole mobility allows charge to be collected faster than in many other active materials [5, 6].

With the intent of providing Elettra's future FOFB with additional information coming from state-of-the-art diamond pBPMs, a diagnostic beamline has been built at the central outlet of one of Elettra's bending magnets. The present document reports on the main features of the implemented line and it's performances.

DIAGNOSTIC LINE

In order to continuously monitor the photon beam without interfering with normal beamline operations, the mentioned diagnostic line exploits one of the central dead-end outlets, which had been arranged at each bending magnet of the Elettra synchrotron. The prototype beamline has been accommodated inside the shielding wall of the storage ring, between the pipes of lines 10.1L and 10.1R, as shown in Fig. 1; this has imposed stringent room constraints, which have been met thanks to the compact size of the diamond pBPMs.

The line features an overall length of about 5 m and it is hooked up to the stopper chamber of the 10.1 front end through a 2-mm-thick water-cooled aluminium window, approximately 4 m downstream from the source point. Due to its geometry, the window accepts about 1 mrad (horizontally) of the beam cone. Moreover, it separates the UHV of the storage ring from the vacuum of the demonstrator and it serves as X-ray filter to reduce the heat load on the detectors. Half meter downstream the Al window, a remotely controlled beam shutter is situated, which allows blocking the beam whenever it is required. Other 80 cm further downstream, a motorized slit system is incorporated, which allows the beam to be shaped and cleaned in horizontal and vertical direction, respectively.

ISBN: 978-3-95450-132-8 doi:10.18429/JACoW-IPAC2014-THPME128

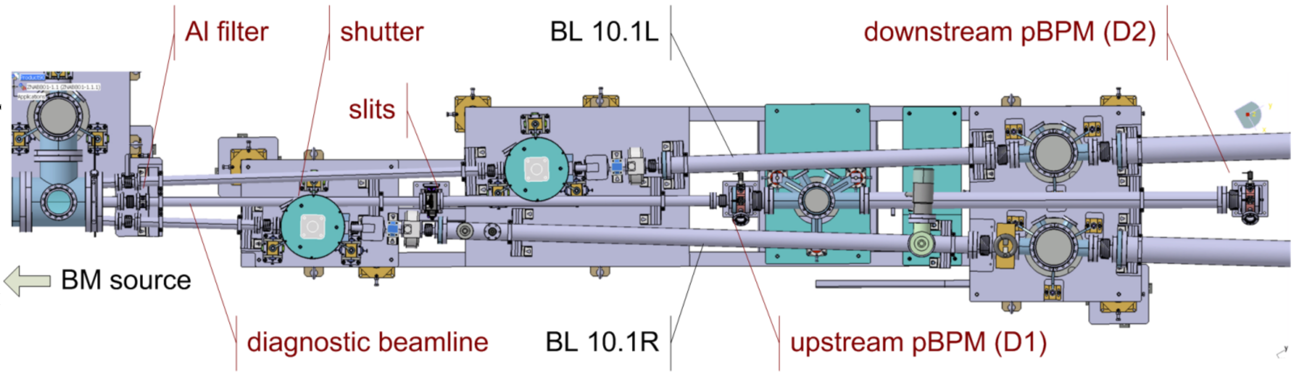

Figure 1: Top view of bending-magnet front end 10.1 at Elettra. The diagnostic beamline is represented by the central pipe between beamlines 10.1L and 10.1R. The main components are labelled in red (upstream to downstream, i.e. left to right): Al filter, beam shutter, motorized slits, upstream pBPM (D1), downstream pBPM (D2).

The upstream pBPM (D1) is placed 1.3 m upstream from the slits (i.e. 6.6 m from the source), followed by the downstream pBPM, which is 2.4 m apart from it (i.e. 9 m from the source). Outside the shielding wall, a PC-based control system allows acquiring and processing pBPM data for testing and beam monitoring through a convenient graphical user interface. Furthermore, it controls motors and biasing modules, allowing for both detector realignment and beam shaping.

DIAMOND-BASED PHOTON BPMS

The upstream pBPM is based on a 50-µm-thick, freestanding, single-crystal CVD diamond. This sensor is a 4.7×4.7 mm^2 die, mechanically grinded and lapped from a 500-µm-thick base material. Front and back surfaces have been coated with 100-nm-thick Al electrodes on top of 100-nm-thick diamond-like-carbon layers. A four-quadrants (*quad*) structure has been created by segmenting the front electrode through a lithographic process, leaving a 100-µm-wide gap between quadrants.

The sensor of the downstream pBPM differs from D1 in terms of thickness and electrode material. It consists of a standard, 500-µm-thick, single-crystal CVD diamond coated with Cr-Au electrodes. It features the same area and quad geometry as D1. The lower thickness of D1 reduces its absorption, allowing most of the photons through towards D2.

Each of these devices is glued and wire-bonded onto a printed-circuit carrier board and mounted on an X-Y movable stage, which is, in turn, housed in a CF-63-flanged, UHV-compatible chamber. These carrier boards are electrically connected via BNC and SMA feedthroughs for biasing and readout, respectively. Such readouts are then fed into AH501B picoammeters[1] in order to acquire the photo-generated currents. While these instruments allow the signals to be sampled at a maximum rate of 6.5 kHz, the diamond pBPMs described above can detect incoming photons with much higher time resolutions; in principle, they are capable of monitoring SR beams on a bunch-by-bunch basis, even at a 500-MHz repetition rate [7].

1http://iloweb.elettra.eu/index.php?page=_layout_prodotto&id=141&lang=en

PERFORMANCES

In order to evaluate the position-encoding capabilities of the system, some preliminary characterizations have been carried out. The slit aperture has been fixed to 300×300 µm^2; with such setup, the system works in a *camera obscura* configuration. Mesh and linear scans of the detectors have been performed during normal machine operations.

D2 has been moved with respect to the stationary photon beam by utilizing the stepper motors coming with detector chamber. At a sampling rate of 10 Hz the pBPM has estimated the relative beam displacement (with *difference-over-sum* method) with a precision of 124 nm. As shown in Fig. 2, the linear range extends for approximately 400 µm.

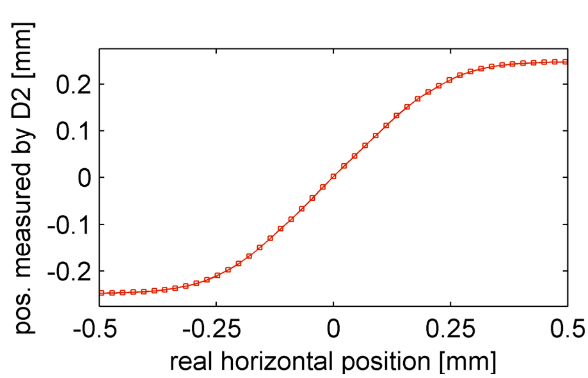

Figure 2: Horizontal position estimated by D2 during a horizontal translation of its movable stage.

In this case, to a first approximation, the 10-kHz precision can be estimated in 3.9 µm. With a 10-Hz acquisition rate, a precision of 72 nm is theoretically expected in such conditions. However, it must be pointed out that the acquired data are dominated by systematic

ISBN: 978-3-95450-132-8 doi:10.18429/JACoW-IPAC2014-THPME128

errors such as stepping precision, slow beam movements, etc.

Analogous linear scans have been performed during dedicated shifts by deliberately moving the electron beam while keeping the detectors in position. In this case, the position estimated by D2 has shown a similar trend, except for a quasi-periodic deviation (of about 15 µm peak to peak) from the linear interpolation. Since in such bending-magnet section the electron-beam position is not directly measurable with the eBPMs, it is estimated through a non-linear fit on the simulated optics. Thus, the recorded deviations might be imputed to the position-estimation algorithm used by the control system of the machine. This would be also in good agreement with the step width by which the electron beam has been moved (30 µm) as related to the spatial-frequency content of the deviations.

It is worth mentioning that, due to the small vertical emission angle (about 100 µrad at 2 GeV), the slit aperture cuts specific portions out of the Gaussian vertical beam profile. This turns into a significant flux decrease for wide vertical beam movements and, as a consequence, a reduction in precision. In future, the vertical aperture is likely to be increased in order to avoid these effects; in such case, the vertical position has to be estimated by the combined readings of D1 and D2.

Test at a 6.5-kHz sampling rate have also been carried out during normal machine operations (2 GeV, 300 mA). A typical trace of the vertical position estimated by D2 is reported in Fig. 3 along with its Fast Fourier Transform (FFT).

A periodic pattern with a σ_{RMS} of about 2 µm is prominent and superimposed with a stochastic uncertainty of about 500 nm, which can be considered as the resolution limit for the system at the aforementioned frame rate and photon flux. The FFT reveals a number of systematic components contributing to such fluctuations. In particular, significant contributions at 17 Hz and 23.5 Hz (imputable to water cooling) are visible; besides this, 100-Hz fluctuations and harmonics are prominent (noise from correctors).

For what concerns intensity monitoring, the photon flux can be directly estimated through the sum of the acquired photo-currents. With a machine current of 300 mA this gives 20 nA and 0.19 µA for D1 and D2, respectively, with a precision better than 1%. Since only sparse data on radiation damage of this kind of CVDs caused by long-term exposure with x-rays is available in literature, the demonstrator was operated continuously over a period of 6 months. The total current remained reasonably constant over the span of time with respect to a given machine energy; this is an important point with a view to future applications of CVDs in FOFB systems.

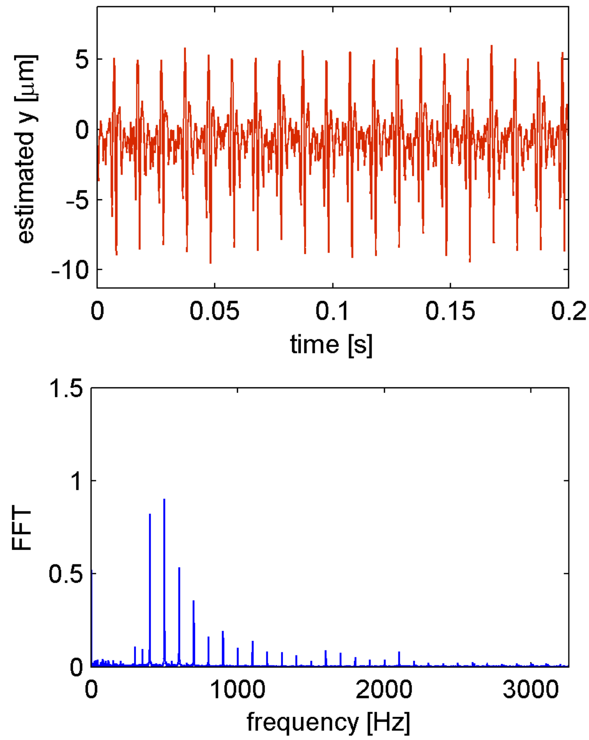

Figure 3: Vertical position estimated by D2 at a sampling rate of 6.5 kHz (top) and corresponding FFT (bottom).

CONCLUSIONS

In its first 6 months of operation the diagnostic-line demonstrator has turned out to be a reliable instrument, allowing for surveillance of bending-magnet radiation with high relative intensity resolution (better 1%) and high position resolution (better than 1 µm) at a maximum frame rate of 6.5 kHz. In order to include these diamond-based pBPMs in a FOFB system, the maximum frame rate should be increased to 10 kHz; this requires some refinements on the readout electronics, which can be implemented without major problems.

REFERENCES

[1] A. Galimberti et al., Nuclear Instruments and Methods A 477, 317 (2002).
[2] M. Lonza et al., Proceedings of the 10th ICALEPCS, Geneva, Switzerland, PO2.011-2, 2005.
[3] T. Scarvie et al., Infrared Physics & Technology 45, 403 (2004).
[4] T. Schilcher et al., Proceedings of DIPAC'05, Lyon, France, POW015, 2005.
[5] J. Morse et al., Journal Synchrotron Radiation 17, 456 (2010).
[6] M. Antonelli et al., Proceedings of SPIE 8504, San Diego, USA, 85040D, 2012.
[7] M. Antonelli et al., Nuclear Instruments and Methods A 730, 164 (2013).